Cell, Vol. 104, 709–718, March 9, 2001, Copyright ©2001 by Cell Press

Conserved Role of a Complement-like Protein in Phagocytosis Revealed by dsRNA Knockout in Cultured Cells of the Mosquito, *Anopheles gambiae*

Elena A. Levashina,*§ Luis F. Moita,*§ Stephanie Blandin,* Gert Vriend,* Marie Lagueux,† and Fotis C. Kafatos*‡
*EMBL
1 Meyerhofstrasse
69117 Heidelberg
Germany
†UPR 9022 du CNRS
IBMC
15 rue René Descartes
67084 Strasbourg Cedex
France

Summary

We characterize a novel hemocyte-specific acute phase glycoprotein from the malaria vector, *Anopheles gambiae*. It shows substantial structural and functional similarities, including the highly conserved thioester motif, to both a central component of mammalian complement system, factor C3, and to a panprotease inhibitor, α_2-macroglobulin. Most importantly, this protein serves as a complement-like opsonin and promotes phagocytosis of some Gram-negative bacteria in a mosquito hemocyte-like cell line. Chemical inactivation by methylamine and depletion by double-stranded RNA knockout demonstrate that this function is dependent on the internal thioester bond. This evidence of a complement-like function in a protostome animal adds substantially to the accumulating evidence of a common ancestry of immune defenses in insects and vertebrates.

Introduction

Mosquitoes, like other insects, display powerful humoral and cellular defense reactions that help fight bacterial and parasite infections and are reminiscent of innate immune responses in vertebrates (Hoffmann et al., 1999). The humoral responses are best characterized, and a diverse set of immune-inducible genes has been identified. For example, antimicrobial peptides are produced after bacterial challenge, mainly by the mosquito fat body, and are secreted into the hemolymph (reviewed by Dimopoulos et al., 2001). Although the exact role of these genes in the antiparasitic response has not yet been elucidated, they may be involved in vector refractoriness to the parasite (Lowenberger et al., 1999). Cellular responses, which are not as well understood at the molecular level as the humoral defenses, include phagocytosis of bacteria and melanotic encapsulation of larger parasites (reviewed by Barillas-Mury et al., 2000).

‡To whom correspondence should be addressed (e-mail: kafatos@embl-heidelberg.de).
§These authors contributed equally to this work.

We are interested in the molecular mechanisms of recognition and activation of immune effector responses in the mosquito. The local activation of encapsulation reactions and the minimal surface characteristics that are required for recognition of foreign bodies (Gorman et al., 1998) suggest that recognition could rely on a complement-like reaction. In vertebrates, the complement system is a major effector system of innate immunity. It can be activated through three distinct pathways, classical, lectin, and alternative (reviewed by Volanakis, 1998), which intersect at the central component, C3. In all three pathways, proteolytic activation of C3 leads to covalent attachment of a C3 cleavage product through a thioester bond to the pathogen surface, followed by phagocytosis or cell lysis of pathogens. Recent cloning of C3-like molecules from an ascidian protochordate (Nonaka and Azumi, 1999) and a sea urchin (Al-Sharif et al., 1998), and the identification of related *t*hioester-containing *p*rotein (TEP) sequences in *Drosophila melanogaster* (Lagueux et al., 2000), prompted us to search for members of the same family in the most important insect vector of human malaria, *Anopheles gambiae*.

Here we report the identification and functional characterization of a novel *Anopheles* TEP (aTEP-I), which shows significant sequence similarity both to vertebrate complement factors and to the related family of animal α_2-macroglobulins (α_2M). aTEP-I is a hemocyte-specific acute phase glycoprotein, which is proteolytically processed in mosquito hemolymph shortly after septic injury. Studies on a hemocyte-like mosquito cell line reveal that aTEP-I can bind to *Escherichia coli* and *Staphylococcus aureus* and that this binding is dependent on a functional thioester bond. Finally, double-stranded RNA (dsRNA) knockout experiments demonstrate that this complement-like protein strongly promotes phagocytosis of three tested Gram-negative bacteria in a mosquito cell line. In contrast, phagocytosis of the Gram-positive *S. aureus* and two other bacterial species was consistently low and not significantly affected by the aTEP-I knockout, suggesting that additional molecules are required to promote uptake of Gram-positive bacteria.

Results

Cloning and Characterization of *aTEP-I*

To clone *TEP* sequences of *A. gambiae*, we designed degenerate primers corresponding to the highly conserved thioester site of the related genes of *D. melanogaster*. PCR experiments with a degenerate *TEP* primer and a T7 primer from the ZAP Express vector on a pool of cDNAs of the mosquito cell line 5.1* (Danielli et al., 2000) yielded a 1.6 kb 3′ sequence of a novel gene, which displayed sequence similarity with C3 and α_2M. 5′-RACE PCR amplified 1.5 kb of additional 5′ sequence, which was used as a probe to screen a 5′-enriched thoracic cDNA library (Arca et al., 1999). A 4.2 kb clone, *aTEP-I*, was isolated and contained a complete open reading frame of 1340 amino acids.

The translated sequence of aTEP-I was aligned with

sequences of representative thioester-containing proteins using the program CLUSTAL_X. The overall sequence similarity was approximately 22%. Furthermore, clustered matches of high identity were distributed along the molecule, leaving no doubt that aTEP-I is a member of the thioester-containing protein family. The predicted organization of aTEP-I is compared with that of human α_2M and C3 in Figure 1A. The aTEP-I sequence contains a signal peptide-like hydrophobic N-terminal segment suggesting that, like other TEPs, it is a secreted protein. The canonical thioester motif (GCGEQ) (red star) is located at a comparable position in all three molecules (residues 858–862 in aTEP-I).

The thioester proteins show distinct preferences in their binding activities, related to a histidine residue about 100 amino acids downstream of the thioester site. In C3, His favors the formation of ester bonds with hydroxyl groups of carbohydrates whereas in α_2M, its absence leads to preferential formation of amide bonds with free amino groups of proteins (reviewed by Dodds and Law, 1998). Interestingly, in aTEP-I, a presumed catalytic His is found at the same site (position 972, blue asterisk).

A clear difference between C3 and α_2M is their post-synthetic intracellular processing. C3 is split into two chains, α and β, which are held together by disulfide bridges, while α_2Ms function as dimers or tetramers of intact chains (reviewed by Sottrup-Jensen, 1989). No clear-cut site (RRRR/RKKR) for this type of processing into two chains has been identified in aTEP-I, indicating that the molecule may be secreted as a single chain polypeptide. Subsequent limited extracellular proteolysis at centrally located sites activates the secreted TEPs. In human C3, a cleavage site (RS) (Figure 1A, black arrow) separates anaphylatoxin (purple) from the C-terminal effector region. Similarly, α_2M recognizes proteases through a particularly exposed peptide stretch (bait region, green). In aTEP-I, a region enriched in potential cleavage sites RX or KX (X = S, A, K, L, V) is indicated in red.

A cluster of six cysteine residues at the C terminus of aTEP-I (Figure 1A) forms a signature that is shared with *Drosophila* TEPs (Lagueux et al., 2000) but is absent from α_2M and complement factors. Otherwise, cysteines are not numerous in insect TEPs (ten in total in aTEP-I), and are not in conserved locations relative to the much more numerous cysteines of vertebrate TEPs. Potential N-glycosylation sites are found both in insect and vertebrate TEP sequences (Figure 1A, black asterisks). Neglecting potential posttranslational modifications, the calculated molecular mass of the secreted aTEP-I protein is 149.957 kDa.

Phylogenetic Analysis of aTEP-I and Related Thioester-Containing Proteins

The availability of insect TEPs from two different insect species and our detection of two nearly identical TEP sequences in the *Caenorhabditis elegans* WORMPEP database permitted us to perform a phylogenetic analysis of the animal TEP family across more than a billion years of evolution. The overall sequence similarity of aTEP-I to the C3, C4, and C5 complement factors and to α_2M ranged from 21 to 24%, while the similarity in

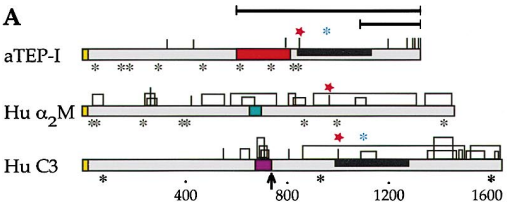

B

Sequences	Hu C3	Su C3	Hu α2M	Li α2M	aTEP-I	
Hu C3		**30.4**	**26.2**	**29.5**	**25.5**	C3d region
Su C3	*24.6*		**27.8**	**29.3**	**25.5**	
Hu α2M	*23.6*	*22.7*		**40.3**	**28.6**	
Li α2M	*22.9*	*21.9*	*31*		**32.6**	
aTEP-I	*23.3*	*21.3*	*22.8*	*23.7*		
	Full-length					

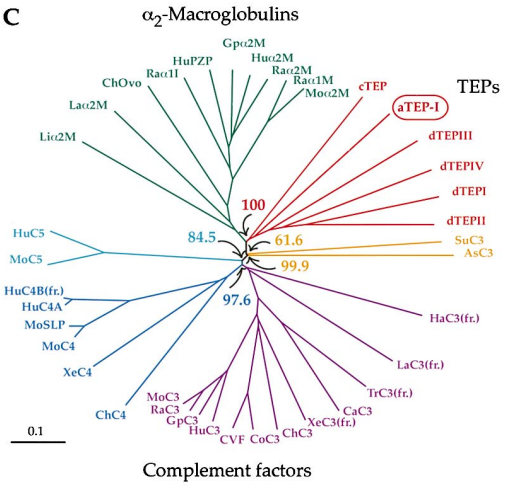

Figure 1. Sequence Comparison and Phylogenetic Tree of Thioester-Containing Proteins

(A) Schematic representation of thioester-containing proteins: *A. gambiae* aTEP-I (accession number AF291654) and human (Hu) C3 and α_2-macroglobulin. Thick marks indicate cysteines connected into the known disulfide bridges of C3 and α_2M. Red stars point to the internal β-cysteinyl-γ-glutamyl thioester sites. Blue asterisks show catalytic histidines and black asterisks are putative N-glycosylation sites. The color-filled segments indicate: yellow, signal peptide; red, a region containing putative protease cleavage sites for aTEP-I; green, the bait region of α_2M; violet, anaphylatoxin C3a; black half-filled segments, C3d region in C3 and its equivalent in aTEP-I. Black vertical arrow shows the C3 activation site. Numbers correspond to amino acid positions. Black horizontal bars show the aTEP-I fragments that were used as antigens for antibody production.

(B) Matrix of percentage amino acid similarity in the aligned full-length sequences (italics) and in the critical C3d-like region (bold) between representative members of the thioester-containing protein family.

(C) Unrooted phylogenetic tree of thioester-containing proteins. The tree was built by the neighbor-joining method based on the alignment of the sequences using CLUSTAL_X. Alignment and sequence information is accessible online. The insect/nematode TEP clade is colored red; the complement C3, C4, and C5 clades are violet, blue, and light blue, respectively; the α_2-macroglobulin clade is green; and the outbranching ascidian and sea urchin C3 factors are in orange. Bootstrap values of 1000 replicates (%) are for the nodes indicated by arrows.

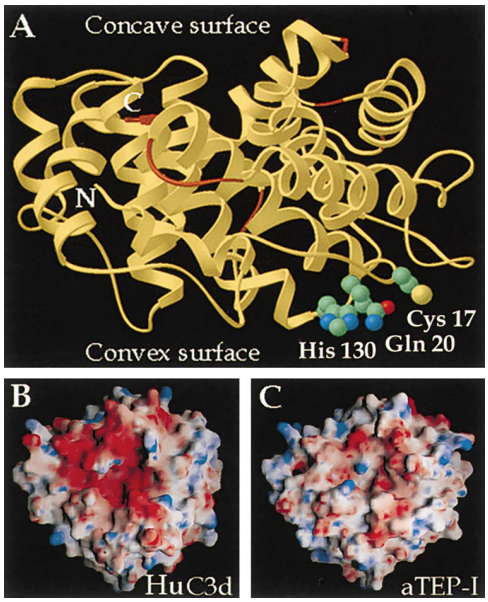

Figure 2. Modeling of the C3d-like Region of aTEP-I

(A) Ribbon model of aTEP-I. Areas that differ from the human C3d structure are colored in brown. The side chains of critical residues (Cys and Gln of the thioester site and a catalytic His) are shown as ball-and-stick models (C, green; N, blue; O, red; S, yellow).

(B and C) Comparison of electrostatic potential maps of concave surfaces between human C3d (B) and the aTEP-I model (C). Maps were built with GRASP (Nicholls et al., 1991). The potential range is from −10.011 (dark red) to +10.045 (dark blue).

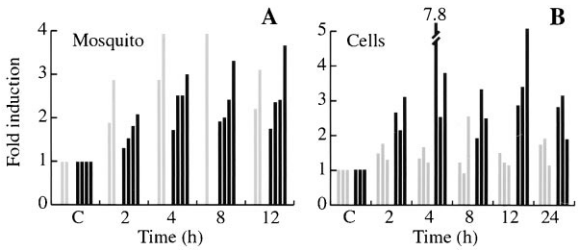

Figure 3. Immune-Inducible Transcription of *aTEP-I*

Semi-quantitative RT-PCR was performed and the levels of the aTEP-I transcript were normalized relative to the internal control transcript for ribosomal protein S7. Quantification was done by fluorimager using SYBR green fluorescent dye. (A) Immune challenge of nonfed (gray bars) and bloodfed (black bars) females with a live mix of *E. coli* and *M. luteus*. (B) Incubation of the 5.1* cell line with heat-killed bacteria: gray bars, *M. luteus*, black bars, *E. coli*. Results of independent experiments are shown as fold induction relative to the unchallenged control (C) at various time points after immune challenge (2 to 24 hr).

the most conserved region (C3d-like, see below) ranged from 26 to 32% (Figure 1B).

Based on the full-length multisequence alignment built with CLUSTAL_X, we constructed an unrooted phylogenetic tree using the neighbor-joining method (Figure 1C). Insect TEPs formed a new clade in this family, intermediate between the clade of α_2M (from vertebrates and the horseshoe crab *Limulus*) and the clades of complement factors (vertebrate C3, C4, and C5, and the outlying ascidian and sea urchin C3). Interestingly, the *C. elegans* TEP clustered with the insect TEP clade, within which the four molecularly characterized dTEPs form deep branches. The same topology was observed for the phylogenetic tree based on the alignment of the C3d-like regions (data not shown). Thus, insect/worm TEPs may represent a primitive but diversified group of TEP sequences, distinct from both complement factors and α_2M.

Modeling of a Critical aTEP-I Region

Initial information about structural features of aTEP-I and their functional implications was gained by homology-based modeling of a region of aTEP-I corresponding to the thioester-containing C3d fragment of human C3 (Figure 1A, black half-filled segment). In the structure of human C3d (Nagar et al., 1998), the critical residues (Cys, Gln, and His) involved in the formation and catalytic activation of the thioester bond are clustered in and protrude from the convex surface (Figure 2A). The opposite, concave surface of C3d serves as the recognition site for complement receptor CR2. The C3d structure and the corresponding aTEP-I model are remarkably similar, except for the unmatched C terminus and four short nonhelical segments (brown in Figure 2A). In particular, the critical reactive and catalytic residues are similarly clustered at the convex surface. This and the very high conservation of surrounding residues (not shown) strongly suggest that aTEP-I is able to form a functional thioester bond very similar to C3. In contrast, the concave surfaces are different in electrostatic maps: the C3d surface (Figure 2B) shows an extended negatively charged acidic pocket, whereas the core of this surface in aTEP-I (Figure 2C) is hydrophobic and is surrounded by a hydrophilic region.

Transcriptional Profiles of *aTEP-I*

Thioester-containing proteins are often acute phase proteins (reviewed by Volanakis, 1995). The immune-responsiveness of *aTEP-I* was analyzed in female mosquitoes after poking with a mixture of live *E. coli* and *Micrococcus luteus*. Bacterial challenge rapidly induced transcription of *aTEP-I*, resulting in maximum transcript levels after 4–6 hr (Figure 3A). Within the adult, *aTEP-I* expression showed a pattern often associated with hemocytes and fat body: presence in head, thorax, and abdomen but virtual absence from the midgut (data not shown). Therefore, we investigated the expression of this gene in an immune-responsive, hemocyte-like cell line 5.1* established by H.-M. Müller (Catteruccia et al., 2000a). In this cell line, *aTEP-I* was expressed constitutively at a low level. Presence of heat-killed *E. coli* markedly induced gene expression, which reached a maximum of 4-fold induction at 4–8 hr of incubation (Figure 3B). In contrast, incubation with heat-killed *M. luteus* did not lead to substantial upregulation. These results indicate that *aTEP-I* is an immune-responsive gene, and that in cells in vitro it is responsive to *E. coli*, but not to *M. luteus*.

Protein Profiles of aTEP-I in Development and Immune Response

To detect the aTEP-I protein both biochemically and by immunolocalization, we raised and affinity-purified rabbit and rat polyclonal antibodies directed against a

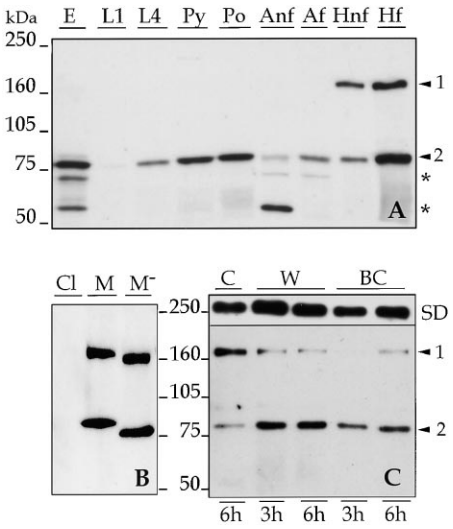

Figure 4. Immunoblotting Analysis of aTEP-I Using 6% SDS-PAGE

(A) Total protein extracts were from embryos (E), first instar larvae (L1), fourth instar larvae (L4), young white pupae (Py), old tanned pupae (Po), nonfed adult females (Anf), and bloodfed adult females (Af). Hemolymph was collected from ten nonfed females (Hnf) and ten bloodfed females (Hf). Total hemolymph extracts and 10–15 μg of total protein from the other extracts (quantified by the Bradford method) were analyzed. Arrowheads 1 and 2 point to putative full-length and cleaved aTEP-I bands, respectively, and asterisks indicate putative proteolytic fragments.

(B) The aTEP-I-positive bands were not detected in mosquito 5.1* cells (Cl) but were abundant in their conditioned medium (M). N-glycosidase F treatment of the conditioned medium (M^-) reduced the sizes of both aTEP-I-positive bands.

(C) Cleavage of aTEP-I protein in the hemolymph of bloodfed adults before (C) and after wounding (W) or bacterial challenge (BC). Hemolymph of ten females was collected at 3 and 6 hr directly into the loading buffer, immunoblotted with anti-aTEP-I rabbit antiserum, and revealed by anti-rabbit HRP-conjugated antibody. The blot was stripped and reprobed with a polyclonal antibody raised against the Sp22D modular protease (Danielli et al., 2000), which served as a loading control (SD). Molecular weight scale (50–250 kDa) is shown on the left.

GST-aTEP-I fusion protein representing two nested C-terminal 21 and 83 kDa polypeptides of aTEP-I (Figure 1A, black horizontal bars). In immunoblotting analysis, both anti-21 kDa and anti-83 kDa antibodies recognized a major protein of 80 kDa in mosquito extracts at all stages of development, as well as smaller moieties, two of which recurred in embryos and adults (arrowhead 2 and two asterisks in Figure 4A, respectively). We interpret these three bands as processed forms of aTEP-I resulting from proteolysis, after which the thioester bond is expected to be rapidly inactivated (reviewed by Dodds and Law, 1998). A bigger, approximately 165 kDa band (Figure 4A, arrowhead 1), interpretable as full-length glycosylated aTEP-I, was abundantly detected only in the hemolymph of adult mosquitoes and, weakly, in embryonic extracts. Interestingly, conditioned medium of 5.1* cell cultures resembled hemolymph in containing both the 165 and 80 kDa bands, while the cells themselves were essentially devoid of aTEP-I (Figure 4B). Treatment of the conditioned medium with N-glycosidase F led to reduction in size of both major bands (Figure 4B), confirming that aTEP-I is a glycosylated protein. Since the 80 kDa moiety is also glycosylated and detected by an antibody directed to the C-terminal region, some of the putative N-glycosylation sites in the vicinity of the thioester site (Figure 1A) are apparently functional. The same protein patterns were observed after SDS-PAGE both in reducing and nonreducing conditions (data not shown). We conclude that aTEP-I is secreted into the hemolymph as a single chain and that fragments generated by subsequent proteolytic cleavages are not connected by disulfide bonds.

We speculated that the proteolytic cleavage of aTEP-I might be inducible by microorganisms or by aseptic injury. To test this, bloodfed females were either challenged by injection of a bacterial mixture or wounded, and 3 or 6 hr later hemolymph was collected and analyzed by immunoblotting. Both wounding and bacterial challenge resulted in cleavage of full-length aTEP-I in hemolymph (Figure 4C). At later time points, we observed replenishment of the 165 kDa form (data not shown).

aTEP-I Is Selectively Expressed in Mosquito Hemocytes

The dispersed association of *aTEP-I* mRNA with head, thorax, and abdomen, the presence of the full-length protein primarily in hemolymph and in conditioned medium of a hemocyte-like cell line suggest that aTEP-I originates in hemocytes. This has been confirmed by immunostaining analysis of body walls: abdomens were dissected open and freed of the alimentary canal (whose epithelium does not itself express significant amounts of aTEP-I; data not shown). aTEP-I was mostly detected in hemocytes attached to tracheae (Figures 5A and 5B) or to the edges of fat body lobes; none was detected in the fat body cells themselves, in the nervous system, in muscles, or in ovaries. Interestingly, the aTEP-I-positive hemocytes (Figure 5C) coexpressed Sp22D (Danielli et al., 2000; Gorman et al., 2000), a hemocyte-specific serine protease (Figures 5D, 5E, and 5F). The only other cells positive for aTEP-I were the pericardial cells (Figure 5G). The putative role of these large binuclear cells in hemolymph filtration and clearance (Hoffmann, 1966; reviewed by Wigglesworth, 1970) suggests that the immunopositive signal may reflect uptake of inactivated aTEP-I rather than in situ synthesis of this protein. Again, aTEP-I and Sp22D were co-detected in the pericardial cells, albeit in different compartments (Figure 5H–5I). aTEP-I was also present in the form of cytoplasmic granules in a small fraction of 5.1* cells, up to 5% of the total, where it colocalized with Sp22D (Figures 5J–5L).

Denaturation-Dependent Fragmentation of aTEP-I

Structure modeling of aTEP-I predicted the functionality of the thioester bond. This internal bond makes known TEP proteins sensitive to denaturation, which causes a cleavage of the peptide bond between the Glu and Gln residues of the thioester site and consequent fragmentation of the molecule; the propensity to fragmentation is abolished by inactivation of the thioester bond through pretreatment with small nucleophilic molecules such as methylamine (MA) (Howard, 1980). Conditioned cell culture medium was collected and treated for 2 hr at 37°C

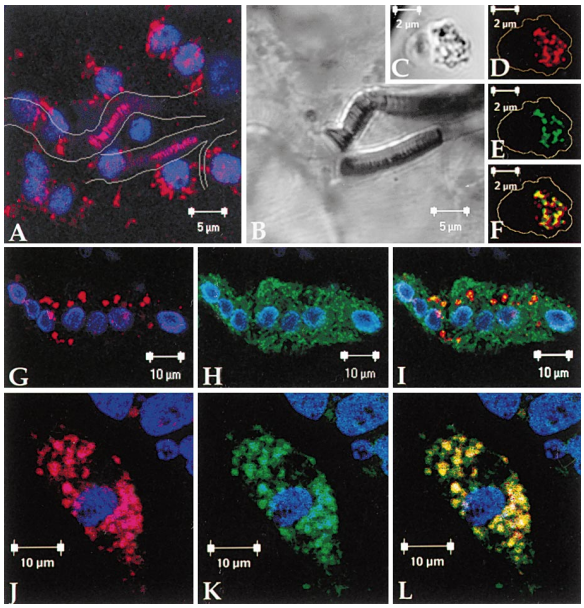

Figure 5. Immunolocalization of aTEP-I in Adult Tissues and a Cell Line

(A–I) Whole mount double staining of adult mosquito body wall showing location of aTEP-I, Sp22D, and nuclear histones (red, green, and blue, respectively). (A) Immunostaining of aTEP-I in hemocytes attached to tracheae, which are traced by thin lines. (B) Phase contrast image of the same field displaying the tracheae. (C) Phase contrast image of a mosquito hemocyte. Coexpression of aTEP-I (D) and Sp22D (E) in a mosquito hemocyte evidenced by merging the images (F). Constitutive presence of aTEP-I (G) and Sp22D (H) in pericardial cells. Note that the merged image (I) reveals that aTEP-I and Sp22D are in separate compartments. Double staining of 5.1* cells for aTEP-I (J) and for Sp22D (K) showing their colocalization in the merge image (L) in the 5.1* cells. Nucleic acids (blue) are colored with TO-PRO™-3.

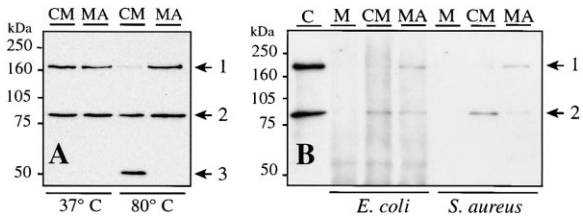

Figure 6. Functionality of the aTEP-I Thioester Site and Its Role in Binding to Bacteria

(A) Denaturation-dependent fragmentation and methylamine reaction of aTEP-I revealed by immunoblotting using 7% SDS-PAGE. Control (CM) and MA-treated (MA) samples of conditioned medium were incubated either at 37°C or at 80°C for 2 hr. Denaturation-induced fragmentation of the control sample occurred at the thioester site, resulting in degradation of full-length aTEP-I (arrow 1) and appearance of a novel 50 kDa band (arrow 3), distinct from the endogenously processed 80 kDa product (arrow 2).

(B) Cell-free conditioned medium of the 5.1* cell line was incubated with (MA) at 0.2 M final concentration or without (CM) methylamine for 2 hr. Fresh medium (M), CM, and MA-treated media were then mixed with the Gram-negative (*E. coli*) or the Gram-positive (*S. aureus*) bacteria for 5 min. The bacteria were centrifuged, washed in PBS, and denatured in 30 μl of reducing buffer at 68°C for 15 min. Aliquots of 15 μl from each sample including the initial conditioned medium (C) were fractionated by 7% SDS-PAGE and immunoblotted as in Figure 4.

with MA solution in PBS (0.2 M final concentration) or with PBS alone. Samples of control or MA-treated media were denatured at 80°C for 2 hr and analyzed by immunoblotting (Figure 6A). Consistent with our interpretation that the 80 kDa band is an inactive processed form lacking the thioester bond, this band was not affected by the treatment. In contrast, heat denaturation of the control sample led to appearance of a novel 50 kDa band with concomitant loss of the 165 kDa full-length protein. This shift required the thioester bond, as it was not observed after MA treatment. The estimated size of the novel 50 kDa band is in reasonable agreement with that predicted (54 kDa) for a denaturation-dependent fragmentation of aTEP-I at the thioester motif.

aTEP-I Binds to Bacteria through the Thioester Bond

In vertebrates, the thioester bond allows complement factors to bind covalently to target surfaces. To investigate whether this is also true for mosquitoes and, specifically, to test for binding of aTEP-I to bacteria, we pretreated aTEP-I containing conditioned medium with or without MA, and then incubated comparable *E. coli* or *S. aureus* preparations in these media. After a 5 min exposure to the media, the bacteria were washed and their cell walls were mildly disrupted by heat denaturation in a reducing buffer. Bacterial pellets and extracted wall protein fractions were analyzed by immunoblotting (data not shown and Figure 6B). A major aTEP-I-positive signal corresponding to the 80 kDa cleaved fragment was detected both in *E. coli* and *S. aureus* cell wall extracts. Importantly, this signal was dramatically reduced in the extracts exposed to MA-treated medium. We conclude that binding of a processed form of aTEP-I to bacteria requires an intact thioester bond. In the same medium, a surprising faint signal corresponding to the full-length form was repeatedly detected.

aTEP-I Is Essential for Promotion of Phagocytosis of Gram-Negative Bacteria in a Mosquito Cell Line

We set up a phagocytic assay to examine whether binding of aTEP-I to bacteria can opsonize them for phagocytosis. We analyzed the propensity of mosquito 5.1* cells to phagocytose fluorescein-labeled bacteria, which had been pre-exposed to either fresh or conditioned culture media for 15 min. Opsonized bacteria were washed and presented to the mosquito cells in internalization medium. At 15 to 60 min, the mosquito cells were collected, treated with ethidium bromide, and plated on slides for fluorescence microscopy (Figures 7A and 7B). Staining with ethidium bromide helps to discriminate between engulfed (green) and surface-attached (orange) bacteria (Drevets and Campbell, 1991). Cells ($n = 100$) were counted in three different fields and the percentage of cells that contained one or more engulfed bacteria was used as the phagocytic index (PI). Bacteria preincubated with fresh culture medium were taken up rather slowly; the PI was only 10.6% at 15 min and reached 40.1% at 60 min, when it approached a plateau (Figure 7C and data not shown). Treatment of

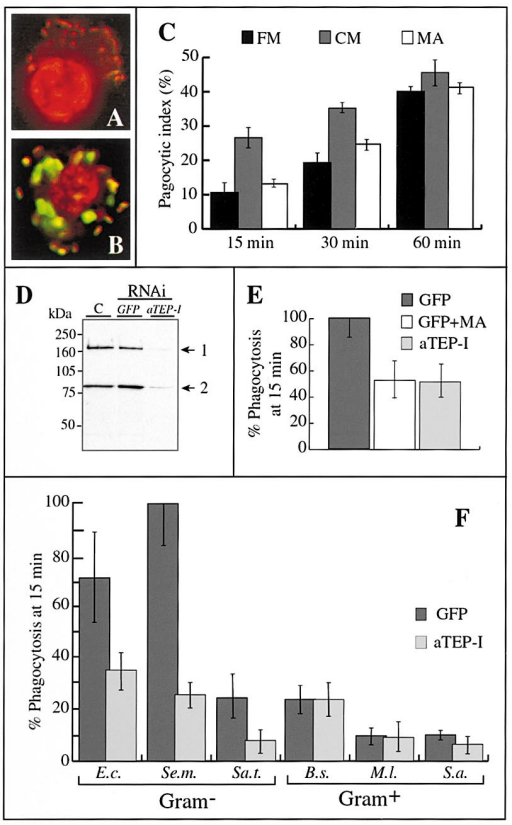

Figure 7. Phagocytosis of FITC-Labeled Bacteria by Mosquito 5.1* Cells

(A and B) Fluorescence microscopy of mosquito phagocytic cells. Treatment with ethidium bromide stains nucleic acids in red. Fluorescein-labeled *E. coli* attached to the cell surface emits in orange (A), whereas engulfed bacteria are colored in green (B).

(C) Phagocytic index (PI) showing the propensity of mosquito 5.1* cells to phagocytose fluorescein-labeled *E. coli* that had been pretreated with fresh medium (FM), conditioned medium (CM), and MA-treated conditioned medium (MA). Opsonized bacteria were washed and presented to naive 5.1* cells in internalization medium for 15, 30, and 60 min.

(D) Knockout of *aTEP-I* by dsRNA interference (RNAi) in mosquito cells. Full-length and processed aTEP-I (arrows 1 and 2) were detected by immunoblotting using 8% SDS-PAGE in control medium (C) and in conditioned medium of cells transfected with 500 ng of *GFP* dsRNA (*GFP*); it was absent from medium of cells transfected with *aTEP-I* dsRNA (*aTEP-I*). Molecular weight scale is on the left.

(E) Effect of *aTEP-I* RNAi knockout on phagocytosis of *E. coli* at 15 min of incubation. Bacterium was opsonized with conditioned medium of the ds(*GFP*) knockout experiments (GFP), with the same medium treated with MA (GFP+MA) and with conditioned medium of ds(*aTEP-I*) knockout (aTEP-I).

(F) Effect of the *aTEP-I* RNAi knockout on the phagocytosis of Gram-negative and Gram-positive bacteria after 15 min of incubation. Comparable preparations (see Experimental Procedures) of *E. coli* (*E.c.*), *Serratia marcescens* (*Se.m.*), *Salmonella typhimurium* (*Sa.t.*), *Bacillus subtilis* (*B.s.*), *Micrococcus luteus* (*M.l.*), and *Staphylococcus aureus* (*S.a.*) were opsonized with the ds(*GFP*) knockout and ds(*aTEP-I*) knockout conditioned media as described above. In (E) and (F), the maximal PI levels were expressed as 100% of phagocytosis. In all graphs vertical bars show mean ± SD (n = 3).

the cells with an inhibitor of actin polymerization, cytochalasin D, or incubation at 4°C drastically inhibited uptake (4 and 1% after 2 hr of incubation, respectively), confirming that the counted events represented phagocytosis rather than actin-independent endocytosis. Preincubation of bacteria with conditioned medium led to precocious phagocytosis (Figure 7C, PI of 27% at 15 min); this phenomenon was still evident at 30 min, but not at 60 min. Thus, the conditioned medium contains soluble factors secreted by 5.1* cells, which opsonize bacteria during the pretreatment and promote phagocytosis.

To address the potential role of mosquito TEPs in promotion of phagocytosis, we inactivated aTEP-I and potentially other aTEPs, present in the conditioned medium by MA treatment. The effect of this treatment on early phagocytosis was spectacular; at 15 min of incubation, the PI was induced only to the level of bacteria preincubated with fresh culture medium, and was 2-fold lower than after pretreatment with normal conditioned medium (Figure 7C). Again, this difference was abolished after 60 min of incubation. These results demonstrate an important role of mosquito TEPs in promoting early phagocytosis.

To specifically deplete aTEP-I from the conditioned medium, we used dsRNA interference (RNAi), which has been recently successfully applied to *Drosophila* cell cultures (Hammond et al., 2000) and is known to inhibit gene expression in a sequence-specific manner (reviewed in Bosher and Labouesse, 2000). Mosquito 5.1* cells were treated with dsRNA representing either a 640 bp 3′ fragment of *aTEP-I* [ds(*aTEP-I*)] or the full-length *GFP* gene [ds(*GFP*)] as a control. Immunoblotting confirmed that the level of aTEP-I was dramatically reduced in the ds(*aTEP-I*) medium, whereas it was present in the ds(*GFP*) medium at the control level (Figure 7D). The specific depletion of aTEP-I from the conditioned medium had a striking effect on phagocytosis of *E. coli* at 15 min of incubation; it reduced the PI to a level as low as that for the MA-treated conditioned medium of the ds(*GFP*) knockout (Figure 7E).

The observation that aTEP-I was essential for opsonization and promotion of phagocytosis of *E. coli* in the hemocyte-like mosquito cell line led us to examine opsonic properties of this protein in phagocytosis of other Gram-negative and Gram-positive bacteria. We followed the scheme described above and compared the PIs of 5.1* cells 15 min after incubation with bacteria opsonized with the conditioned media of ds(*GFP*) or ds(*aTEP-I*) knockout. The highest PI was detected for *Serratia marcescens* and we have expressed it as 100% of phagocytosis (Figure 7F). Phagocytosis of all three species of Gram-negative bacteria was reduced by 50%–75% when microorganisms were opsonized with aTEP-I-depleted medium. Strikingly, the 5.1* cells showed only low levels of phagocytic activity against three species of Gram-positive bacteria, and this activity was not affected by the aTEP-I knockout. These results suggest that aTEP-I promotes phagocytosis of some Gram-negative bacteria, but is not sufficient to promote the uptake by 5.1* cells of any of the three tested species of Gram-positive bacteria.

Discussion

The complement system was thought to be an exclusive hallmark of the host defense of vertebrates until C3-

like molecules were recently cloned in nonvertebrate deuterostomes, a sea urchin (Al-Sharif et al., 1998) and an ascidian (Nonaka and Azumi, 1999). Although thioester proteins had been described in protostomes (Armstrong and Quigley, 1987; Kopacek et al., 2000), they appeared to exhibit α_2-macroglobulin-like protease inhibitory activities rather than complement-like properties. In this report, we present the first functional evidence that a protostome, the mosquito *Anopheles gambiae,* expresses a thioester-containing protein that resembles complement in promoting phagocytosis. Our results, therefore, indicate that the complement-like proteins have a much longer history than previously thought and can be traced back to dipteran insects.

At the structural level, aTEP-I exhibits specific features of both C3 and α_2M, suggesting that it has retained ancient properties of both and may be a prototype of their common ancestor molecule. For example, our modeling studies point to a high conservation of key residues between C3 and aTEP-I on the convex surface of the respective C3d-like regions, although here the sequence similarity does not exceed 25.5%. In contrast, the corresponding region of α_2M from *Limulus*, which shows 32.6% of similarity to aTEP-I and 29.5% to human C3d, has structurally diverged and cannot be modeled successfully using the C3d structure as a template (data not shown). The structural conservation of the C3d-like region of C3 and aTEP-I probably reflects shared functional requirements for covalent attachment of these molecules to microbial surfaces. In keeping with this, we observed that the characteristic complement-like properties of aTEP-I, such as the attachment to bacteria and the subsequent promoting of precocious phagocytosis, are both dependent on the functional thioester bond.

As is the case for α_2M, aTEP-I is secreted as a single chain product. It is tempting to speculate that in these single chain molecules, the bait-like region is exposed in a way that makes it an easy target for a wide variety of activators. In contrast, the two- and three-chain factors C3, C4, and C5 rely on specific convertase complexes for their activation. We propose that activation of insect TEPs, unlike that of complement, does not require such convertase complex. This speculation is supported, albeit negatively, by an extensive search of the fruitfly genome that failed to find such specific complement-activating proteases as MASP or factors B and C2. Taking into account that such activating components of both the lectin and the alternative pathways exist in ascidians (reviewed by Nonaka, 2000), we suggest that these pathways first appeared in protochordate deuterostomes, and that insect TEPs are activated by endogenous proteases that are set free upon injury, or by proteases of pathogen origin. Indeed, our results imply that aTEP-I can be cleaved by endogenous proteases in the hemolymph after injury.

Although we have shown that aTEP-I binds to both *E. coli* and *S. aureus*, preliminary data indicate that it binds poorly to *M. luteus*; thus, the range of its binding specificity remains to be examined. A potential role of aTEP-I in host defense during *Plasmodium* infection was not addressed in this paper. However, preliminary data indicate that this gene responds to the presence of the parasite in the midgut by transcriptional upregulation. Further studies will clarify whether aTEP-I or other members of aTEP family are implicated in antiparasitic responses, since three additional members of the thioester family have been recently identified in *A. gambiae* (E. A. L., L. F. M., and S. B., unpublished data; Dimopoulos et al., 2000; Oduol et al., 2000).

We observed that in the absence of a functional thioester bond, full-length aTEP-I can bind, albeit weakly, to *E. coli* and to *S. aureus*. Similarly, several ELISA-based reports have shown binding of α_2M to pathogens (Araujo-Jorge et al., 1990). These results may indicate that early in evolution, this type of opsonin was able to bind noncovalently to microorganisms without proteolytic activation. We propose that later in evolution, such a primitive opsonization system adopted a proteolytic activation step, concomitant with covalent binding mediated by the thioester bond, and that this evolutionary step permitted a fine-tuning of pathogen recognition coupled to a high-affinity binding to the target.

The cell culture model system based on the hemocyte-like 5.1* cell line proved to be helpful in the establishment of a quantitative phagocytic test for the mosquito. The possibility to specifically inactivate the expression of *aTEP-I* by dsRNA interference demonstrated the importance of aTEP-I in opsonization for phagocytosis of the Gram-negative bacteria, *E. coli*, *S. marcescens*, and *S. typhimurium*. In contrast, the low level of phagocytosis of the Gram-positive bacteria, *B. subtilis*, *M. luteus*, and *S. aureus*, and its independence from the aTEP-I knockout, suggest that aTEP-I is not sufficient to promote phagocytosis of this latter type of bacteria in these cells. Thus, this in vitro cell culture model has provided a first insight into the complexity of the phagocytic system in mosquitoes and can potentially serve to further dissect the molecules involved in regulation of phagocytosis.

The bacteria binding and phagocytosis-promoting activities of aTEP-I clearly define this protein as an opsonin for some Gram-negative bacteria. Opsonization is thought to be the most conserved function of thioester-containing proteins (reviewed by Dodds and Law, 1998), and the discovery of an opsonizing insect TEP is important evidence favoring this concept. The predominant hemocyte origin of aTEP-I and the ability of this glycoprotein to promote phagocytosis by the hemocyte-like 5.1* cells highlight the role of hemocytes in the innate defense system of *Anopheles*. Several recent reports have pointed to the importance of insect hemocytes in providing interaction between cellular and humoral immune responses (Basset et al., 2000; Elrod-Erickson et al., 2000; Schneider and Shahabuddin, 2000). It is not clear whether aTEP-I is the only mosquito opsonin that promotes phagocytosis of Gram-negative bacteria. The effect of chemical inactivation or of RNAi depletion of aTEP-I is most striking at early time points of phagocytosis, which may suggest that additional opsonins can promote phagocytosis at later stages. An alternative explanation for the later leveling off of the differences between fresh and conditioned media may be the accumulation of newly synthesized aTEP-I, or, most likely, opsonin-independent internalization.

Finally, this report presents a successful application of double-stranded RNA interference using a cell culture model system to study gene function in mosquito, where

in vivo genetic analysis cannot be applied. This technique, in conjunction with subsequent validation by the very demanding method of genetic transformation of anopheline mosquitoes (Catteruccia et al., 2000b), opens up the possibility of functionally characterizing genes involved in complex phenotypes, such as the immune responses in vector insects.

Experimental Procedures

Biological Material

Mosquito colonies were maintained as described (Richman et al., 1997). Young adult nonfed and bloodfed females were injured with a thin needle (0.2 mm diameter) or infected by a needle dipped into a concentrated overnight culture of *Escherichia coli* strain 1106 and *Micrococcus luteus* strain A270. The Sua 5.1* cell line was cultured and incubated with heat-killed *E. coli* or *M. luteus* as described (Müller et al., 1999).

Cloning and Sequencing

Using a primer F2: 5′-GGITGYGGIGAGCAGAATATG-3′ corresponding to the thioester motif and a reverse primer T7: 5′-TAATACGACT CACTATAGGG-3′, a 1.6 kb PCR product was amplified from a lambda ZAP express (Stratagene) cell line cDNA library, cloned into pGEM-TA easy vector (Promega), and confirmed by sequencing. RACE-PCR using a specific primer: 5′-GTGCGGCCCGCTACGG TAGCG-3′ and the Marathon Kit (Clontech) produced a 1.5 kb fragment, which was used for screening a thoracic cDNA library (Arca et al., 1999). A clone of 4.2 kb was sequenced by Eurogentec (Herstal, Belgium) and analyzed using the SMART and BLAST programs.

Modeling of a Critical aTEP-I Region

The alignment of aTEP-I with C3d was performed by CLUSTAL_X and refined by introducing corresponding regions of other TEP sequences. The WHAT IF program (Vriend, 1990) was used for modeling as described (Chinea et al., 1995). Sequence identity between the template and the aTEP-I model was 25.5%. The model quality was checked with WHAT IF structure validation tools (Rodriguez et al., 1998). The sequence alignment and the coordinates of the model are available online.

Transcriptional Profiling by RT-PCR

Total RNA from adult mosquitoes and cultured cells was isolated with TRIZOL Reagent (Gibco BRL) according to the suppliers' instructions. First strand cDNA synthesis was performed as described (Müller et al., 1999). The aTEP-I primers 5′-GGAAATACCGGAGGA CAC-3′ and 5′-TGCTACCTTAAAGCGTCTG-3′ were used at 10 pmol per 25 μl PCR reactions to amplify a 409 bp fragment with a standard program (30 s at 94°C; 30 s at 56°C; 60 s at 72°C) for 25 cycles (cDNA from adults) or 32 cycles (cDNA from cells). The internal S7 control (Salazar et al., 1993) was amplified using 19 cycles of the same program. The linear range of all amplification reactions has been determined empirically. After electrophoresis on 1% agarose, gels were stained with the SYBR green dye (Molecular Probes) for 1 hr and analyzed with a fluorimager (Fuji).

Generation and Immunopurification of aTEP-I Antibody

Chimeric proteins composed of glutathione S-transferase (GST) and the C-terminal regions of aTEP-I were produced using the GST-aTEP-I vectors pLL2 and pLL4. For pLL2, a BamHI-XhoI 2351 bp fragment of *aTEP-I* cDNA was cloned into corresponding sites of the pGEX-3T expression vector (Frorath et al., 1992). For pLL4, a HindIII-XhoI 680 bp fragment was first subcloned into the pBluescript KS vector, and then recloned as a 705 bp BamHI-XhoI fragment into pGEX-3T. Fusion proteins were expressed in *E. coli* strain BL 21 and purified according to standard procedures (Pharmacia) on a glutathione Sepharose 4B column. For each protein, two rats and two rabbits were immunized with 50 μg protein per rat and 250 μg protein per rabbit using R-700 and R-730 adjuvants, respectively (RIBI Immunochem Research, Inc.). Rats were boosted every third week with 50 μg antigen until final bleed. Rabbits were boosted every fourth week with 250 μg antigen for 6 months. Identical protein profiles were detected by immunoblotting using antibodies directed against the pLL2 and pLL4 fusion proteins. Rabbit antibody against the pLL4 protein was affinity-purified using FPLC-purified antigen bound to activated CNBr Sepharose 4B beads as described (Harlow and Lane, 1988).

Immunoblotting

Protein extracts from adults, hemolymph collection, and immunoblotting were performed as described (Danielli et al., 2000). In all experiments, aTEP-I antiserum was used at 1:1,000 dilution. Bound antibodies were detected by an anti-rabbit IgG conjugated to horseradish peroxidase (Promega) at 1:40,000 using Western Blot Chemiluminescence Reagent Plus Kit (NEN™ Life Science Products). Protein loading and efficiency of protein transfer were monitored by blot staining with Indian ink (Harlow and Lane, 1988). Asparagine-linked glycan chains on aTEP-I were cleaved using the N-Glycosidase F Deglycosylation Kit (Roche Molecular Biochemicals) according to a standard protocol, with 5 μl of conditioned medium incubated for 15 min with or without N-glycosidase F (1 μl) at 37°C, followed by immunoblotting.

Immunostaining

Whole mount and cell line staining was performed as described (Danielli et al., 2000). Briefly, after blocking, the body walls were incubated overnight at 4°C with a mixture of primary antibodies [aTEP-I at 1:750, Sp22D at 1:1,000 and histone (MAB052, Chemicon) at 1:500] followed by 1 hr incubation with secondary antibodies (The Jackson Laboratory, 1:1,000). The samples were analyzed with a Zeiss LSM 510 confocal microscope. Cell line nuclei were colored with TO-PRO™-3 (Molecular Probes, 1:1,000) for 15 min.

Binding Assay

Conditioned media of 5.1* cell line were incubated with or without MA (0.2 M final concentration) for 2 hr at 37°C. Comparable preparations of chemically inactivated *E. coli* (K-12 strain) and *S. aureus* BioParticles®, fluorescein conjugate (Molecular Probes) were incubated for 5 min with the conditioned media, centrifuged, washed with PBS, and treated with 30 μl of denaturation buffer (Rosenbusch, 1974). After 15 min at 68°C the reactions were separated into soluble and nonsoluble fractions and analyzed by immunoblotting.

dsRNA Production and Interference

For the production of dsRNA, we modified the pBluescript-based pLL6 plasmid (a gift of T. Loukeris, EMBL, Heidelberg), which contained the full 721 bp *GFP* sequence between EcoRI and ApaI sites, by inserting a second T7 promoter in reverse orientation between the SstI and SstII. The resulting pLL6ds plasmid was used to produce a control *GFP* dsRNA. For producing *aTEP-I* dsRNA, the *GFP* fragment was exchanged for the 661 bp fragment of pLL4 using SmaI-KpnI sites of pLL6ds resulting in pLL17. Purified linearized plasmids served as templates for RNA synthesis using the MEGASCRIPT T7 transcription kit (Ambion). RNAs were isopropanol precipitated, quantified, and mixed for annealing in equal quantities by heating for 5 min at 95°C and cooling down to room temperature. Resulting dsRNAs were analyzed on agarose gel. In interference experiments, 500 ng of each dsRNA was transfected into a confluent culture of 5.1* cells using the Effectene Transfection Reagent (Qiagen) following the manufacturers' instructions. The conditioned media were exchanged for a fresh medium after 2 days. Samples for immunoblotting and phagocytic assay were collected 5 days later.

Phagocytic Assay

Cells and conditioned media (1- to 2-week-old) of the 5.1* mosquito confluent cell cultures (Catteruccia et al., 2000a) were used. Three bacterial species were comparable commercial preparations (Molecular Probes): BioParticles®, fluorescein conjugates *E. coli* (K-12 strain) and *S. aureus* (Molecular Probes) and *S. marcescens* (custom prepared by the manufacturer). Overnight cultures of *Salmonella typhimurium*, *Bacillus subtilis* (provided as cultures by P. Bulet, IBMC, Strasbourg), and *M. luteus* were prepared in a consistent manner. Bacteria were killed by a 30 min incubation with 4% formaldehyde (Polysciences, Inc.), washed in PBS, and fluorescein conjugated (Drevets and Campbell, 1991). All bacteria were incubated

with the conditioned media for 15 min, washed in PBS, and presented to mosquito cells (in a ratio of 20:1, respectively) in internalization medium consisting of 10 mM HEPES, 5 mM glucose in MEM (SEROMED®), pH 7.4. The phagocytic test was adapted from Drevets and Campbell (1991). All experiments were performed at least three times.

Acknowledgments

We thank Professor J. A. Hoffmann for initial support and constant interest in the work, A. Danielli and T. G. Loukeris for fruitful discussions, T. Gibson for help with the phylogenetic analysis, and H.-M. Müller for the 5.1* cell line. This work was supported by NIH program project (1PO1 AI44220) and European Commission Training and Mobility of Researchers Program (ERB4061PL95) grants. E. A. L. is a fellow of the European Molecular Biology Organization.

Received September 7, 2000; revised January 18, 2001.

References

Al-Sharif, W.Z., Sunyer, J.O., Lambris, J.D., and Smith, L.C. (1998). Sea urchin coelomocytes specifically express a homologue of the complement component C3. J. Immunol. *160*, 2983–2997.

Araujo-Jorge, T.C., de Meirelles, M. de N., and Isaac, L. (1990). *Trypanosoma cruzi*: killing and enhanced uptake by resident peritoneal macrophages treated with alpha-2-macroglobulin. Parasitol. Res. *76*, 545–552.

Arca, B., Lombardo, F., de Lara Capurro, M., della Torre, A., Dimopoulos, G., James, A.A., and Coluzzi, M. (1999). Trapping cDNAs encoding secreted proteins from the salivary glands of the malaria vector *Anopheles gambiae*. Proc. Natl. Acad. Sci. USA *96*, 1516–1521.

Armstrong, P.B., and Quigley, J.P. (1987). Limulus alpha 2-macroglobulin. First evidence in an invertebrate for a protein containing an internal thiol ester bond. Biochem. J. *248*, 703–707.

Barillas-Mury, C., Wizel, B., and Soo Han, Y. (2000). Mosquito immune responses and malaria transmission: lessons from insect model systems and implications for vertebrate innate immunity and vaccine development. Insect Biochem. Mol. Biol. *30*, 429–442.

Basset, A., Khush, R.S., Braun, A., Gardan, L., Boccard, F., Hoffmann, J.A., and Lemaitre, B. (2000). The phytopathogenic bacteria *Erwinia carotovora* infects *Drosophila* and activates an immune response. Proc. Natl. Acad. Sci. USA *97*, 3376–3381.

Bosher, J.M., and Labouesse, M. (2000). RNA interference: genetic wand and genetic watchdog. Nat. Cell Biol. *2*, E31–E36.

Catteruccia, F., Nolan, T., Blass, C., Müller, H.M., Crisanti, A., Kafatos, F.C., and Loukeris, T.G. (2000a). Toward *Anopheles* transformation: Minos element activity in anopheline cells and embryos. Proc. Natl. Acad. Sci. USA *97*, 2157–2162.

Catteruccia, F., Nolan, T., Loukeris, T.G., Blass, C., Savakis, C., Kafatos, F.C., and Crisanti, A. (2000b). Stable germline transformation of the malaria mosquito *Anopheles stephensi*. Nature *405*, 959–962.

Chinea, G., Padron, G., Hooft, R.W., Sander, C., and Vriend, G. (1995). The use of position-specific rotamers in model building by homology. Proteins *23*, 415–421.

Danielli, A., Loukeris, T.G., Lagueux, M., Müller, H.M., Richman, A., and Kafatos, F.C. (2000). A modular chitin-binding protease associated with hemocytes and hemolymph in the mosquito *Anopheles gambiae*. Proc. Natl. Acad. Sci. USA *97*, 7136–7141.

Dimopoulos, G., Casavant, T.L., Chang, S., Scheetz, T., Roberts, C., Donohue, M., Schultz, J., Benes, V., Bork, P., Ansorge, W., et al. (2000). *Anopheles gambiae* pilot gene discovery project: identification of mosquito innate immunity genes from expressed sequence tags generated from immune-competent cell lines. Proc. Natl. Acad. Sci. USA *97*, 6619–6624.

Dimopoulos, G., Müller, H.M., Levashina, E.A., and Kafatos, F.C. (2001). Innate immune defense against malaria infection in the mosquito. Curr. Opin. Immunol. *13*, 79–88.

Dodds, A.W., and Law, S.K. (1998). The phylogeny and evolution of the thioester bond-containing proteins C3, C4 and alpha 2-macroglobulin. Immunol. Rev. *166*, 15–26.

Drevets, D.A., and Campbell, P.A. (1991). Macrophage phagocytosis: use of fluorescence microscopy to distinguish between extracellular and intracellular bacteria. J. Immunol. Methods *142*, 31–38.

Elrod-Erickson, M., Mishra, S., and Schneider, D. (2000). Interactions between the cellular and humoral immune responses in *Drosophila*. Curr. Biol. *10*, 781–784.

Frorath, B., Abney, C.C., Berthold, H., Scanarini, M., and Northemann, W. (1992). Production of recombinant rat interleukin-6 in *Escherichia coli* using a novel highly efficient expression vector pGEX-3T. Biotechniques *12*, 558–563.

Gorman, M.J., Schwartz, A.M., and Paskewitz, S. (1998). The role of surface characteristics in eliciting humoral encapsulation of foreign bodies in Plasmodium-refractory and -susceptible strains of *Anopheles gambiae*. J. Insect. Physiol. *44*, 947–954.

Gorman, M.J., Andreeva, O.V., and Paskewitz, S.M. (2000). Sp22D: a multidomain serine protease with a putative role in insect immunity. Gene *251*, 9–17.

Hammond, S.M., Bernstein, E., Beach, D., and Hannon, G.J. (2000). An RNA-directed nuclease mediates post-transcriptional gene silencing in *Drosophila* cells. Nature *404*, 293–296.

Harlow, E., and Lane, D. (1988). Antibodies: a Laboratory Manual (Cold Spring Harbor, NY: Cold Spring Harbor Laboratory Press).

Hoffmann, J.A. (1966). Etude ultrastructurale de l'absorption de saccharate de fer par les cellules pericardiales de *Locusta migratoria* (Orthoptere). C. R. Acad. Sci. Hebd. Seances Acad. Sci. D *262*, 1471–1496.

Hoffmann, J.A., Kafatos, F.C., Janeway, C.A., and Ezekowitz, R.A. (1999). Phylogenetic perspectives in innate immunity. Science *284*, 1313–1318.

Howard, J.B. (1980). Methylamine reaction and denaturation-dependent fragmentation of complement component 3. Comparison with alpha2-macroglobulin. J. Biol. Chem. *255*, 7082–7084.

Kopacek, P., Weise, C., Saravanan, T., Vitova, K., and Grubhoffer, L. (2000). Characterization of an alpha-macroglobulin-like glycoprotein isolated from the plasma of the soft tick *Ornithodoros moubata*. Eur. J. Biochem. *267*, 465–475.

Lagueux, M., Perrodou, E., Levashina, E.A., Capovilla, M., and Hoffmann, J.A. (2000). Constitutive expression of a complement-like protein in Toll and JAK gain-of-function mutants of *Drosophila*. Proc. Natl. Acad. Sci. USA *97*, 11427–11432.

Lowenberger, C.A., Kamal, S., Chiles, J., Paskewitz, S., Bulet, P., Hoffmann, J.A., and Christensen, B.M. (1999). Mosquito-*Plasmodium* interactions in response to immune activation of the vector. Exp. Parasitol. *91*, 59–69.

Müller, H.M., Dimopoulos, G., Blass, C., and Kafatos, F.C. (1999). A hemocyte-like cell line established from the malaria vector *Anopheles gambiae* expresses six prophenoloxidase genes. J. Biol. Chem. *274*, 11727–11735.

Nagar, B., Jones, R.G., Diefenbach, R.J., Isenman, D.E., and Rini, J.M. (1998). X-ray crystal structure of C3d: a C3 fragment and ligand for complement receptor *2*. Science *280*, 1277–1281.

Nicholls, A., Sharp, K.A., and Honig, B. (1991). Protein folding and association: insights from the interfacial and thermodynamic properties of hydrocarbons. Proteins *11*, 281–296.

Nonaka, M. (2000). Origin and evolution of the complement system. In Origin and Evolution of the Vertebrate Immune System, L. Du Pasquier and G.W. Litman, eds. (Springer Verlag), pp. 37–50.

Nonaka, M., and Azumi, K. (1999). Opsonic complement system of the solitary ascidian, *Halocynthia roretzi*. Dev. Comp. Immunol. *23*, 421–427.

Oduol, F., Xu, J., Niare, O., Natarajan, R., and Vernick, K.D. (2000). Genes identified by an expression screen of the vector mosquito *Anopheles gambiae* display differential molecular immune response to malaria parasites and bacteria. Proc. Natl. Acad. Sci. USA *97*, 11397–11402.

Richman, A.M., Dimopoulos, G., Seeley, D., and Kafatos, F.C. (1997).

Plasmodium activates the innate immune response of *Anopheles gambiae* mosquitoes. EMBO J. *16*, 6114–6119.

Rodriguez, R., Chinea, G., Lopez, N., Pons, T., and Vriend, G. (1998). Homology modeling, model and software evaluation: three related resources. Bioinformatics *14*, 523–528.

Rosenbusch, J.P. (1974). Characterization of the major envelope protein from *Escherichia coli*. Regular arrangement on the peptidoglycan and unusual dodecyl sulfate binding. J. Biol. Chem. *249*, 8019–8029.

Salazar, C.E., Mills-Hamm, D., Kumar, V., and Collins, F.H. (1993). Sequence of a cDNA from the mosquito *Anopheles gambiae* encoding a homologue of human ribosomal protein S7. Nucleic Acids Res. *21*, 4147.

Schneider, D., and Shahabuddin, M. (2000). Malaria parasite development in a *Drosophila* model. Science *288*, 2376–2379.

Sottrup-Jensen, L. (1989). Alpha-macroglobulins: structure, shape, and mechanism of proteinase complex formation. J. Biol. Chem. *264*, 11539–11542.

Volanakis, J.E. (1995). Transcriptional regulation of complement genes. Annu. Rev. Immunol. *13*, 277–305.

Volanakis, J.E. (1998). Overview of the complement system. In The Human Complement System in Health and Disease, J.E. Volanakis, and M.M. Frank, eds. (New York: Marcel Dekker, Inc.), pp. 9–32.

Vriend, G. (1990). WHAT IF: a molecular modeling and drug design program. J. Mol. Graph. *8*, 52–56.

Wigglesworth, V.B. (1970). The pericardial cells of insects: analogue of the reticuloendothelial system. J Reticuloendothel. Soc. *7*, 208–216.

GenBank Accession Number

The GenBank accession number for the aTEP- I sequence reported in this paper is AF291654. For additional information, see http://www.embl-heidelberg.de/ExternalInfo/kafatos/publications/TEP.